Prediction of SWCC for Coarse Soils Considering Pore Size Changes

Xu Li and Limin Zhang

Department of Civil Engineering, The Hong Kong University of Science and Technology, Clear Water Bay, Hong Kong lixu@ust.hk, cezhangl@ust.hk

Summary. The soil water characteristic curve (SWCC) of a soil is often predicted from the pore size distribution (PSD) of the soil. Experiments show that the PSD may change in the drying or wetting process. It is necessary to consider the pore-size distribution changes in predicting SWCCs.

In this research, different grain-size proportions of completely decomposed granite were separated and then mixed artificially to obtain five soil specimens of different grain-size distributions. These specimens vary from gravel to sand, and silty clay. The SWCCs of these specimens were measured using the axis-translation technique and a Dewpoint psychrometer; and the PSDs of these soil specimens were measured using a mercury intrusion porosimetry (MIP) method. The PSDs obtained from the MIP tests were used to predict the SWCCs, which were compared with the experimental results further.

The PSDs of each soil sample at full saturation and at the end of the SWCC drying test were compared. The PSDs showed a considerable pore-size reduction after soil drying. This phenomenon is referred to as 'pore shrinkage'. A model proposed by Simms and Yanful (2001) was adopted to consider the shrinkage influence in the prediction of the drying SWCC from the PSDs of saturated and dried soil samples. After applying this model, the predicted SWCCs were closer to the experimental SWCCs, especially for fine soils.

For coarse soils, the pore volume with pore diameter larger than a specific value that cannot be measured by MIP tests is large. This volume was estimated and used to correct the predicted SWCC for each coarse soil. With this correction, the predicted SWCCs for coarse soils were also close to the experimental SWCCs.

Key words: SWCC modelling, PSD, pore shrinkage

Introduction

The measurement of soil–water characteristic curve (SWCC) is often time consuming. A traditional method of determining the SWCC using a pressure plate is limited in a narrow suction range. A viable method is to predict SWCC from the pore-size distribution (PSD) of soil.

The nitrogen adsorption and the mercury intrusion porosimetry (MIP) can give PSD curve quantitatively. However, the MIP method has been widely used as a reliable method to measure PSDs of a wide variety of porous solids (Aung et al. 2001). The PSD as measured by MIP has often been advanced as a parameter to help interpret geotechnical behaviors. It has been correlated with saturated hydraulic conductivity (Lapierre et al. 1990), frost heave (Reed et al. 1979), macroscopic volume change (Al-Mukhtar et al. 1996) and SWCC (Prapaharan et al. 1985, Romero et al. 1998).

Based on the PSD from MIP tests, a SWCC can be estimated rapidly in a much wider suction range comparing with the traditional method of determining the SWCC using a pressure plate. But the methodology is still not mature and satisfactory (Simms and Yanful 2004). For example, the PSD changes with soil water content even for a same soil sample. Also, the SWCC prediction method based on the PSD from MIP tests are seldom applied to coarse soils.

Four coarse soils and one fine soil were used in this paper. To investigate the changes in PSD during the soil drying process, a series of MIP tests had been conducted. Also scanning electron microscopy (SEM) tests were used to study the pore geometry of soils qualitatively. Based on the PSDs from the MIP tests, the SWCCs for five soils were predicted with the consideration of the changes of PSD during soil drying and the pore volumes with pore diameters larger than a specific value, which could not be measured in the MIP tests. The predicted SWCCs were further compared with the SWCCs from laboratory tests, which were measured by a pressure plate and a Dewpoint psychrometer.

Materials

Two unimodal soils, one fine soil with an average particle diameter d_{50} of 0.0185 mm and one coarse soil with d_{50} of 6 mm, were 'brewed' from a natural completely decomposed granite (CDG), which was taken from a construction site located at Beacon Hill, Hong Kong. The grain-size distribution (GSD) curves and the grain density function curves are shown in Fig. 1. Firstly, the natural soil was sieved into ten portions according to particle diameter, namely $<$ 0.063 mm, 0.063–0.125 mm, 0.125–0.185 mm, 0.185–0.6 mm, 0.6–2 mm, 2–4.25 mm, 4.25–6 mm, 6–10 mm, 10–14 mm and 14–20 mm. The grain-size distribution of the finest soil–particle portion, which had a maximum soil–particle diameter of 0.063 mm, was measured by the hydrometer tests (BS 1377, part 2. 1990). Secondly, a fine soil was mixed from the finest particle portion with particle diameters smaller than 0.063 mm and the particle portion with particle diameters in range of 0.063–0.125 mm by weight proportions of 0.72 and 0.28. Thirdly, a coarse soil was mixed from all the particle portions following the design GSD (refer to Fig. 1).

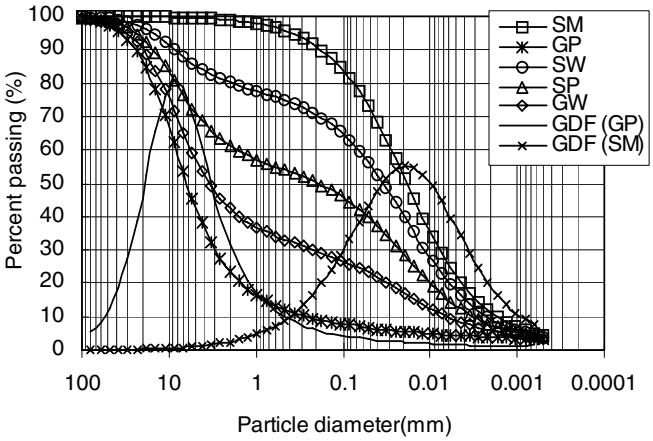

Fig. 1. Grain size distributions of design soils

Further, the fine soil and the coarse soil were mixed into three new soils according to three weight proportions, namely 75% coarse soil mixed with 25% fine soil, 50% coarse soil mixed with 50% fine soil and 25% coarse soil mixed with 75% fine soil.

Basic parameters of these soils were measured and are shown in Table 1. Four types of soil samples were used in the experiments: compacted soil sample (CS), first compacted and then saturated soil sample (SS), oven-dried soil sample (OS) and powder sample (PS). The relative compaction (RC) value, which is defined as the ratio of the dry density to the maximum dry density, was chosen to indicate the soil compaction state.

Table 1. Detailed parameters of five design soils

Soil type	Maximum dry density (g/cm^3)	Optimum water content (%)	Grain size distribution Clay (%)	Silt (%)	Sand (%)	Gravel (%)	Group symbols (ASTM D2487)
1	1.97	9	3.9	3.1	16.7	76.3	GP
2	1.96	11	5.9	18.7	17.9	57.5	GW
3	1.90	13	7.9	34.3	19.1	38.7	SP
4	1.71	18	9.9	49.9	20.3	19.9	SW
5	1.55	21	11.9	65.5	21.5	1.1	SM

Experimental Methods

Scanning Electron Microscopy Tests

SEM was used to study the soil fabric for SM qualitatively. Based on the photographs from the backscattered electron scanning images, the macro-micro fabric at the soil surface could be recognized.

Mercury Intrusion Porosimetry Tests

MIP is routinely and effectively used to evaluate the PSDs of powder and bulk materials with open and interconnected pore structures. Compacted and saturated soil samples (SS) and the oven-dried samples (OS) of five soils (SM, SW, SP, GW and GP) were used to study the changes in PSDs before and after soil drying.

During a MIP test, a dehydrated sample was initially surrounded with mercury at a specific low pressure. Then the surrounded mercury pressure was increased in steps until it reached the system maximum capacity and the intruded volumes of mercury were measured for each pressure increment.

The largest soil sample was limited to 15 cm^3 in the MIP tests. To maintain the homogeneity of soil samples, soil particles with diameters above 10 mm were taken out from the soil when preparing the soil samples for the MIP tests. With the assumption that the remaining part retained the void ratio and PSD of the soil, the density of the soil sample used in the MIP tests was corrected as,

$$\rho_c = \frac{(1-p)\rho}{1-\frac{p\rho}{G_s}} \tag{1}$$

where

ρ = initial soil density;

ρ_c = corrected soil density;

p = weight proportion of the soil particles with diameters larger than 10 mm;

G_s = gravimetric density of the soil solid.

Soil Water Characteristic Curve Tests

The SWCCs of five soils (SM, SW, SP, GW and GP) were measured in the laboratory.

Three devices, a Fredlund SWCC device, a 5-Bar pressure plate extractor and a Dewpoint psychrometer were used to measure the SWCCs. The Fredlund SWCC device was used to measure the wetting and drying SWCC in the suction range of 0–500 kPa. It is similar to traditional one-dimensional pressure plate extractors. The 5-Bar pressure plate extractor was used to measure the drying SWCC in the suction range of 0–500 kPa. With a large sample

container, 300 mm in diameter and 150 mm in height, it is able to measure the SWCCs of large size soil samples and is suitable for coarse soils. The Dewpoint psychrometer was only suitable for measuring the SWCCs of small soil samples or powder soil samples, because of the small sample container, 20 mm in diameter and 12 mm in height. The suction range of the Dewpoint psychrometer was above 500 kPa with an accuracy of ±100 kPa.

Prediction of SWCC Based on the PSD Obtained from MIP Tests

The measured PSD from the MIP tests was used to predict the SWCC. Assuming the pore geometry can be modeled as a bundle of cylindrical tubes, the pore radius r can be calculated by using Jurin's equation (Hillel 1980)

$$r = \frac{2T_{s,\text{water}} \cos \alpha_{\text{water}}}{\psi} = \frac{2T_{s,\text{mercury}} \cos \alpha_{\text{mercury}}}{P} \tag{2}$$

where

ψ = matric suction;
P = mercury injected pressure;
r = entrance pore radius;
$T_{s,\text{water}}$ = surface tension at the water–air interface;
$T_{s,\text{mercury}}$ = surface tension at the mercury–air interface;
α_{water} = contact angle of water–air interface to solid;
α_{mercury} = contact angle of mercury–air interface to solid.

In equation (2), the constants, air/water surface tension $T_{s,\text{water}}$ and mercury/air surface tension $T_{s,\text{mercury}}$ decreased with temperature. For water in contact with air, $T_{s,\text{water}} = 74.2\,\text{mN/m}^2$ at 10°C, $72.0\,\text{mN/m}^2$ at 25°C, and $62.6\,\text{mN/m}^2$ at 80°C. The surface tension of mercury $T_{s,\text{mercury}}$, $472\,\text{mN/m}^2$ at 20°C, is much higher.

Using the symbols used by Simms and Yanful (2002), we define

$$\frac{\partial w(\psi)}{\partial \psi} = vf(\psi) \tag{3}$$

where

$w(\psi)$ = total water content of the soil sample with a suction of ψ;
$vf(\psi)$ = volume fraction of water corresponding to a suction range of $\mathrm{d}\psi$.

Transforming soil suction ψ and mercury intrusion pressure P to pore radius r according to equation (2), one obtains

$$vf(\psi) = vf(r) = vf(P)\,. \tag{4}$$

That is to say, the volume fraction $vf(\psi)$ by drainage of water when the suction increases from ψ to $\psi + \mathrm{d}\psi$ is equal to the volume fraction $vf(P)$ by mercury injection when the mercury intrusion pressure increases from P to $P + \mathrm{d}P$. Also the soil drying process corresponds to a mercury intrusion process.

In the MIP test, the start mercury intrusion pressure P_0 is non-zero. The total water content in a soil sample at suction ψ can be written as

$$w(\psi) = w(0) - \int_0^{\psi} vf(\psi) = w_s - \int_0^{P_0} vf(P) - \int_{P_0}^{P} vf(P) \tag{5}$$

where

w_s = saturated water content of a soil sample;

P_0 = started mercury intrusion pressure;

$vf(P)$ = volume fraction of injected mercury at the mercury intrusion pressure of P.

Limited by the mercury injection pressure ranging from 9.3 kPa to 212 MPa, only pores which have entrance diameters ranging from 0.006 μm to 142 μm can be measured in the MIP tests. There may be a considerable volume of pores with pore entrance diameters larger than 142 μm. For a coarse soil, this volume may be large. This volume is also indicated by the water retention capacity in a suction range of 0 to 2 kPa in the SWCC. If the air entry value (AEV) is larger than 2 kPa, the volume will be 0 and can be ignored. This volume can be estimated by the experimental data and used to correct the predicted SWCC. This correction is referred to as 'P_0 correction.'

In the drying SWCC test, water is gradually removed from soil pores by drainage of the liquid phase, accompanied by pore shrinkage. Earlier research shows that soil shrinkage will change the PSD of the soil sample considerably (Simms and Yanful 2001, 2002). Simms and Yanful (2001) offered a method to model the PSD changes during the SWCC tests based on the assumption that the pores shrunk elastically as water drained from the soil. In this paper, this correction to SWCC prediction was exercised referred to as 'shrinkage correction.'

Results and Discussions

Influence of Water Content on the PSD

SEM photos of an SM SS (RC = 0.85) and an SM OS (RC = 0.85), which was first saturated before it is oven-dried, are shown in Fig. 2. There are much fewer macro pores in the OS. This indicates that most of the macro pores disappear in the process of soil drying.

Under the same soil dry density, the saturated soil sample (freezing dehydration method) and the oven dried soil sample were analyzed by MIP. The PSD curves of the SM SS and the SM OS are shown in Fig. 3. The vertical axis of the figure is the volume frequency, which is defined as the partial derivative of the cumulative injected mercury volume with respect to $\log r$. There were much fewer macro pores (larger than 2 μm) in the SM OS than in the SM SS, which is consistent with the SEM photos shown in Fig. 2. This indicates that

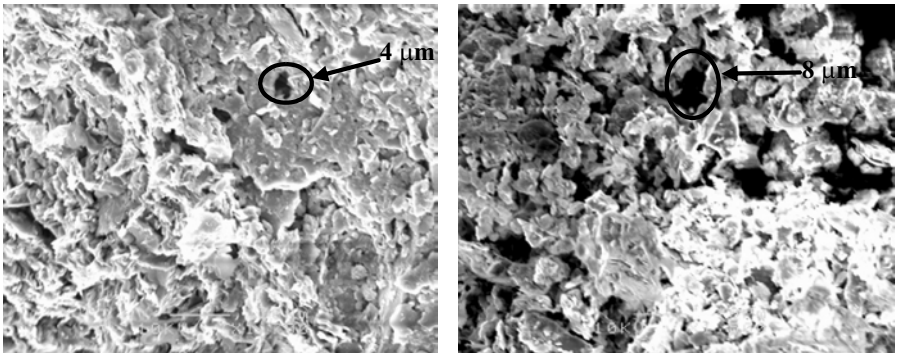

a. Pore geometry of SM OS (RC = 0.85). Scale: 800:1

b. Pore geometry of SM SS (RC = 0.85). Scale: 700:1

Fig. 2. Pore geometry of SM at different water contents

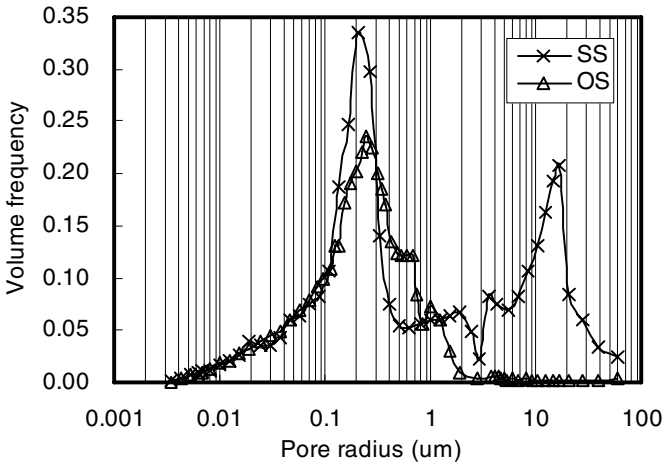

Fig. 3. Pore size distribution curves of SM SS and SM OS (RC = 0.85)

most macro pores with diameter larger than 2 μm disappeared in the drying process of the SM soil sample. A possible reason for this is pore shrinkage. The macro pores may shrink into smaller ones due to the drainage of water in the drying process. At last, only few macro pores are left in the oven-dried SM soil sample. Most of them are surrounded by the smaller pores and cannot be displaced by mercury at low mercury intrusion pressures.

Similar phenomena are found in the comparison of the PSDs of the OS and SS for GP, GW, SP and SW (refer to Fig. 4). General features between the PSD of the SS and the PSD of the OS for a sandy soil or a gravel soil can be summarized as follows:

(1) The PSDs of the SS and the OS are considerably different.

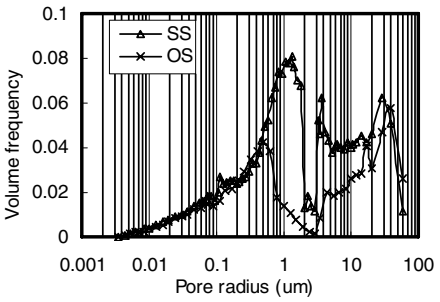

a. Pore size distribution curves for GP

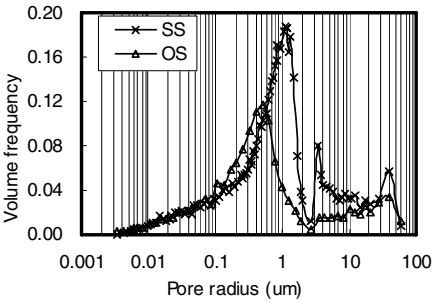

b. Pore size distribution curves for GW

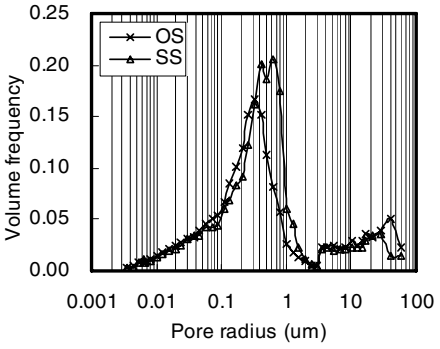

c. Pore size distribution curves for SP

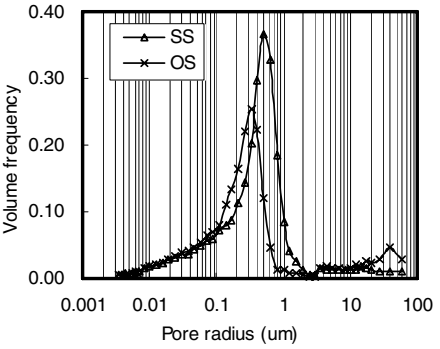

d. Pore size distribution curves for SW

Fig. 4. PSDs of saturated samples and oven-dried samples (RC = 0.85)

(2) Both the PSD of the SS and the OS can be divided into a macro part and a micro part, which has a boundary pore radius of approximately 2 μm. The volume frequencies in the micro part show an obvious peak. The volume frequencies in the macro part are flat without obvious peak.
(3) In the micro part, the peak volume frequency, f_{peak}, and the pore radius at peak volume frequency, r_p, for the SS are larger than those for the OS.
(4) In the micro part, the pores can be divided into three portions by two boundary pore radii r_l and r_u. In the small pore-radius portion, in which the pore radius is smaller than r_l, the volume frequencies of the SS and the OS are same. In the intermediate pore-radius portion, in which the pore radius is larger than r_l but smaller than r_u, the volume frequencies of the SS are smaller than these of the OS. In the large pore-radius portion, in which the pore radius is larger than r_u, the volume frequencies of SS are larger than these of OS.

Features (3) and (4) may be partially induced by shrinkage. If large pores shrunk during the soil drying process, the peak volume frequency and the pore radius at peak volume frequency would decrease. The pore with pore radius

smaller than r_l will not shrink into a smaller one. The upper boundary pore diameter r_u is an apparent radius. The volume of pores with diameter r_u that shrunk from larger pores is equal to the volume of pores with diameter r_u that will shrink into smaller ones. Values of the parameters, f_{peak}, r_p, r_u and r_l were listed in Table 2.

Table 2. Characteristic parameters of PSD for GP, GW, SP and SW

Type of soil sample		r_p (μm)	f_{peak}	r_l (μm)	r_u (μm)
GP, RC = 0.85	SS	1.3	0.080	0.05	0.5
	OS	0.5	0.042		
GW, RC = 0.85	SS	1.1	0.19	0.09	0.7
	OS	0.6	0.12		
SP, RC = 0.85	SS	0.5	0.22	0.04	0.32
	OS	0.23	0.17		
SW, RC = 0.85	SS	0.5	0.37	0.04	0.35
	OS	0.32	0.26		

Notes:
f_{peak} = peak volume frequency in the micro part;
r_p = pore radius at peak volume frequency in the micro part;
r_u = boundary pore radius, above which the volume frequencies of SS were larger than these of OS;
r_l = minimum pore radius of pore shrinkage during soil drainage.

SWCC Prediction Based on the PSD Obtained from MIP Tests

The drying SWCCs of the five soils under the same RC value are put together in Fig. 5. The water retention ability of the five soils increases with the fraction of fine contents in soil.

When the soil suction decreases to 5 kPa, the degrees of saturation of gravel soils, GP and GW, are 0.73 and 0.4. Also the degree of saturation for SW is 0.88 at suction of 5 kPa. That indicates that there are abundant pores with the pore entrance diameter larger than 56 μm (refer to equation (2)). That is to say the pore volume with pore entrance diameter larger than 142 μm for GP, GW and SW, which cannot be measured in MIP tests, should be corrected in the SWCC prediction process. In contrary, the degree of saturation for SM and SP is about 0.99 when the soil suction decreases to 5 kPa. The pore volume with pore entrance diameter larger than 142 μm for SM and SP can be ignored in the SWCC prediction.

The predicted SWCCs of SM are shown in Fig. 6. After the consideration of shrinkage influence (Simms and Yanful 2001), the predicted SWCC is

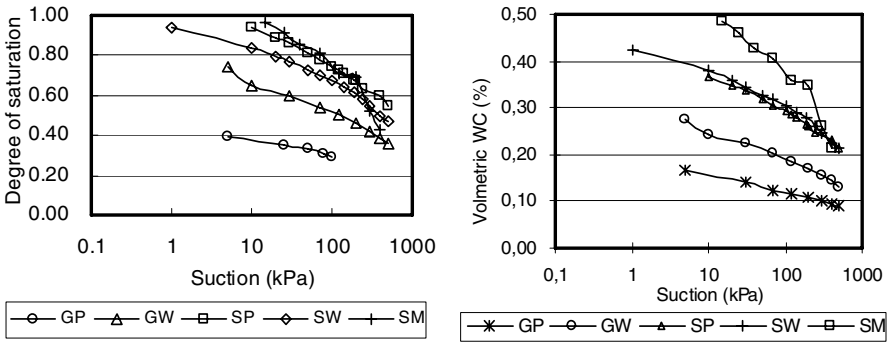

a. Degree of saturation vs. suction

b. Volumetric water content vs. suction

Fig. 5. SWCCs of five soils measured by the soil sample (RC = 0.85)

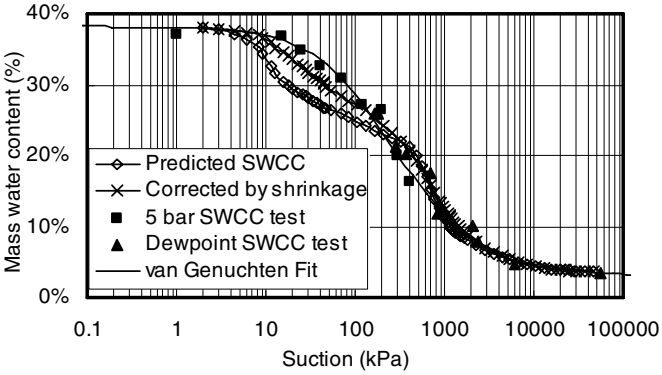

Fig. 6. Predicted SWCCs from PSD for SM (RC = 0.85)

closer to the experiment SWCC. But the predicted AEV, 8 kPa, is less than the AEV from the experiments, 15 kPa. This phenomenon is consistent with Prapaharan et al. (1985) and Simms and Yanful (2001). Prapaharan et al. (1985) gave a possible reason that the clay mineralogy adsorbed to the soil surface and induced a smaller pore diameter at the soil surface in the SWCC tests compared to that in MIP tests. This phenomenon may also be due to the disturbance of the macro pore structures during sample preparation for the MIP tests or due to the inaccuracy of the mercury-air contact angle at the soil surface used in the calculation.

The predicted SWCC for SP is close to that from the experiment (refer to Fig. 7(**a**)). But its shape does not fit the experimental data very well. Also the similarity between the predicted SWCC and the SWCC obtained in the experiment is improved by the shrinkage correction. The P_0 correction is not needed for SP, which is consistent with the experimental SWCCs (refer to Fig. 5(**b**)).

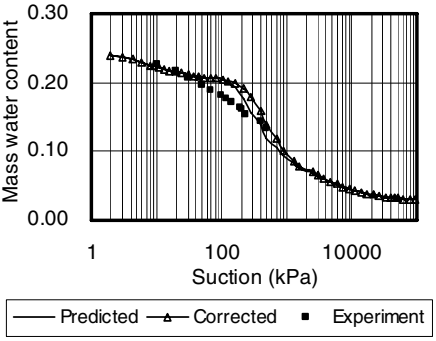

a. Predicted SWCCs from PSD for SP

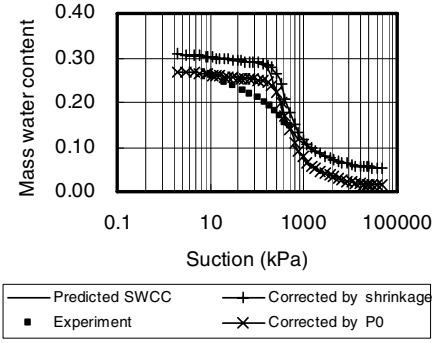

b. Predicted SWCCs from PSD for SW

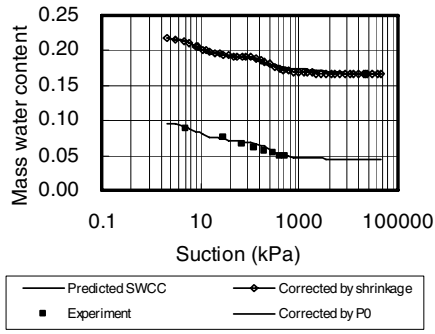

c. Predicted SWCCs from PSD for GP

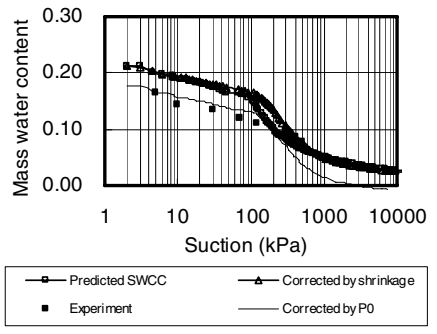

d. Predicted SWCCs from PSD for GW

Fig. 7. Predicted SWCCs from PSDs for GP, GW, SP and SW (RC = 0.85)

The predicted SWCCs from the PSDs of SW, GP and GW are shown in Figs. 7(**b**)–(**d**). Without the P_0 correction, the predicted SWCCs are far away from the experimental SWCCs. With the correction of the pore volume with pore entrance diameters larger than 142 μm, the predicted SWCCs of SW, GP and GW are close to the experimental data. The predicted SWCC of GP is satisfactory. But the shape of the predicted SWCCs of SW and GW are different from that obtained in the SWCC experiments. The influence of shrinkage correction is rather limited for SW, GP and GW.

Summary and Conclusions

A series of MIP tests and SEM tests were conducted in this paper to investigate the changes of PSD during soil drying. Shrinkage phenomena occurred during the drying process for all five CDG soils.

The PSDs obtained from the MIP tests were used to predict the SWCCs of the five soils. The results demonstrated that this method was effective and

could give a drying SWCC rapidly in a much wide suction range. With the P_0 correction, the predicted SWCCs for the coarse soils were close to the experimental SWCCs. With the shrinkage correction, the predicted SWCC for SM fitted the experimental SWCC quite well.

Acknowledgements

This research was substantially supported by a grant from the NSFC/RGC Joint Research Scheme between the National Natural Science Foundation of China and the Research Grants Council of the Hong Kong SAR (Project No. N-HKUST611/03). The authors are grateful to Prof. D. G. Fredlund for constructive discussions during the course of the study.

References

Al-Mukhtar M, Belanteur N, Tessier D, Vanapalli SK (1996) The fabric of clay soil under controlled mechanical and hydraulic stresses, Appl Clay Sci 11:185–197

Aung KK, Rahardjo H, Leong EC, Toll DG (2001) Relationship between porosimetry measurement and Soil water characteristic curve for an unsaturated residual soil, Geotech Geol Eng 19:401–416

Hillel D (1980) Fundamentals of soil physics. Academic Press Inc., London

Lapierre C, Leroueil S, Locat J (1990) Mercury intrusion and permeability of Louisville clay, Can Geotech J 27:761–773

Prapaharan S, Altschaeffl AG, Dempsey BJ (1985) Moisture curve of compacted clay: mercury intrusion method, J Geotech Geoenv Eng 111(9):1139–1143

Reed MA, Lovell CW, Altschaeffl AG, Wood LE (1979) Frost-heaving rate predicted from pore-size distribution, Can Geotech J 16:463–472

Romero E, Gens A, Lloret A (1998) Water permeability, water retention and microstructure of unsaturated Boom clay, Eng Geol 54:117–127

Simms H, Yanful EK (2001) Measurement and estimation of pore shrinkage and pore distribution in a clayey till during soil–water characteristic curve tests, Can Geotech J 38(4):741–754

Simms H, Yanful EK (2002) Predicting soil–water characteristic curves of compacted plastic soils from measured pore-size distributions, Geotechnique 52(4):269–278

Simms H, Yanful EK (2004) Discussion of the application of mercury intrusion porosimetry for the investigation of soils, including an evaluation of its use to estimate volume change in compacted clayey soils, Geotechnique 54(6):421–426